Journal of Applied Polymer Science

Rheological Behavior of Cellulose Nanocrystal Suspension: Influence of Concentration and Aspect Ratio

Qiang Wu,[1,2] Yujie Meng,[2] Siqun Wang,[2] Yanjun Li,[1] Shenyun Fu,[1] Lingfei Ma,[1] David Harper[2]

[1]Department of Wood Science and Technology, College of Engineering, Zhejiang Agricultural and Forestry University, Hangzhou, 311300, China

[2]Center for Renewable Carbon, Department of Forestry, Wildlife & Fisheries, University of Tennessee, Knoxville, Tennessee 37996

Correspondence to: S. Wang (E-mail: swang@utk.edu) and Y. Li (E-mail: lalyj@126.com)

ABSTRACT: The steady and dynamic rheological behaviors of two cellulose nanocrystal (CNC) suspensions were investigated over a wide range of concentrations. The viscosity, storage and loss modules increased with increasing CNC concentration, and both CNC suspensions showed three regions in a viscosity-concentration graph. The two critical concentrations depended on the aspect ratio and corresponded to the overlap and gelation concentration. Because of the higher aspect ratio, switchgrass CNC suspension transitioned into a biphasic state and formed a hydrogel at lower concentrations than those of cotton CNC suspensions. Furthermore, the complex viscosities of both CNC suspensions were higher than their steady viscosities; therefore, neither CNC suspension followed the Cox–Merz rule, which may be attributed to the existence of a liquid crystal domain in each suspension. © 2014 Wiley Periodicals, Inc. J. Appl. Polym. Sci. **2014**, *131*, 40525.

KEYWORDS: cellulose and other wood products; colloids; viscosity and viscoelasticity

Received 8 October 2013; accepted 30 January 2014
DOI: 10.1002/app.40525

INTRODUCTION

Cellulose nanocrystals (CNCs) are conventionally rod-shaped nano-scale entities 5–20 nm in diameter and hundreds or thousands of nm in length that have been isolated from cellulose by acid hydrolysis,[1–3] TEMPO-mediated oxidation,[4–6] enzymatic hydrolysis,[7,8] sono-chemical assisted hydrolysis,[9] ionic liquid method[10] etc. Because of the controllable and convenient treatment, acid hydrolysis is mostly utilized. A series of CNCs have been prepared by acid hydrolysis from different source, such as microcrystalline cellulose,[11] wood,[12] straw,[13,14] bamboo,[15] tunicates,[16,17] switchgrass,[18,19] and many other raw materials. Because of their advantages of having a high modulus, low density, and negligible thermal expansion, CNCs have been widely used as reinforcement in various polymer matrices,[20–27] while pure CNC films have also attracted much attention for their strong antireflective[28] and piezoelectric[29] properties.

Pure CNC materials and CNC/polymer composites are typically prepared by a casting method from CNC suspensions or CNC/polymer solutions; consequently, the rheological behavior of CNC suspensions is of great importance. Bercea and Navard[30] studied the viscosity of aqueous suspensions of tunicate cellulose nanocrystals and found that the phase state of CNC suspension can be determined based on changes in viscosity. Urena-Benavides et al.[31] investigated the rheological behavior of cotton CNC suspension, and found that the phase behavior of CNC suspensions can be divided into four regions with different scaling relationships between rheological parameters and CNC concentrations. Liu et al.[32] and Gong et al.[33] studied the influence of shear rate and temperature on the rheological behavior of CNC hydrogel. Araki et al.[34] and Boluk et al.[35] studied the viscosity of dilute CNC suspension and tried to use Simha formula[36] to calculate CNC's aspect ratio.

The morphology of CNC would influence its diffusion in suspension, and play an important role on rheological behavior of CNC suspension. Aspect ratio is the main character of rod-like CNC, thus, it is an important parameter affecting the rheological behavior of CNC suspensions. However, to our knowledge there are few papers reporting the influence of CNCs' aspect ratio on their steady and dynamic rheological behavior over a wide range of CNC concentration. Therefore, in this study we prepared two kinds of CNCs with different aspect ratios by acid hydrolysis from switchgrass and cotton, and studied the influence of CNCs' aspect ratio on its suspension's steady and dynamic rheological behavior over a wide range of CNC concentrations.

EXPERIMENTAL

Materials

Switchgrass and cotton were chosen as raw materials to prepare CNCs with different morphology. Alamo Switchgrass (*Panicum-virgatum L.*) were obtained from 2011 harvest in East Tennessee. Cotton cellulose filter paper (Whatman 541, England) was milled into powders to prepare the cotton CNC. Switchgrass cellulose was isolated by sequentially removing wax, oil, lignin, and hemicellulose. The switchgrass and cotton CNCs were prepared by sulfuric acid hydrolysis, the procedure was briefly presented as follow. First, switchgrass cellulose (or cotton cellulose) powders were added into sulfuric acid (60 wt %) for hydrolysis at 45°C for 45 min. Then, 10-fold deionized water was added to stop hydrolysis, and the resulting suspensions were centrifuged to remove acid. Afterward, the suspensions were dialyzed with membranes against deionized water until reaching neutral pH. Finally, the suspension was subjected to ultrasonic vibration, and then filtered to remove large pieces of aggregates. The detailed procedure can be seen in our previous studies.[18,19]

Figure 1 shows the AFM images of switchgrass and cotton CNCs. Both CNCs showed a rod-like structure, with the dimensions of length, width and height being 148 ± 42.1, 21 ± 4.3, 3.9 ± 1.3 nm for switchgrass CNCs and 94 ± 31.6, 21 ± 5.5, 7.2 ± 3.0 nm for cotton CNCs, the detail statistical analysis can be seen in our previous study.[18] Because AFM used a non-contact mode, the aspect ratio was estimated as length/height, yielding an aspect ratio of 39 for the switchgrass CNCs and 13 for the cotton CNCs. Given this difference, the two CNCs could then be used to investigate the influence of aspect ratio on the rheological behavior of CNC suspensions.

Preparation of CNC Suspension

To prepare CNC suspensions with accurate concentrations, after dialysis and sonication, the CNC suspensions were freeze-dried (Freezone, LABCONCO, USA) overnight to produce CNC powders. These powders were then added to deionized water and ultrasonicated in an ice bath for 5 min to prepare the CNC suspension concentrations needed for the rheology test. The prepared CNC suspensions were homogenous and no aggregates can be seen by naked eye, the photos of CNC suspensions are shown in Figure 2.

Measurement

Atomic Force Microscopy (AFM) Measurements. The morphology of switchgrass CNC and cotton CNC were characterized by AFM (XE-100, PSIA, Korea). The AFM samples were prepared by depositing a drop of CNC suspension with a concentration of 0.01 wt % onto sheets of freshly cleaved mica that were then dried to remove all water. AFM measurements were performed under ambient conditions. Noncontacted mode was used for this study. Aluminum coated silicon cantilevers with a spring constant of 40 N m^{-1} and resonant frequency of 300 kHz (Nano-science Instruments) was selected, with a conical shaped tip, whose radius of curvature was around 8 nm. AFM Images were scanned at low voltage mode under 0.8 Hz scan rate and 512 pixels by 512 pixels resolution for the purpose of detecting the fine structure. The length, width and height of CNC rods were measured by XEI software, over 120 CNC rods were measured to statistically analyze the CNC dimension.

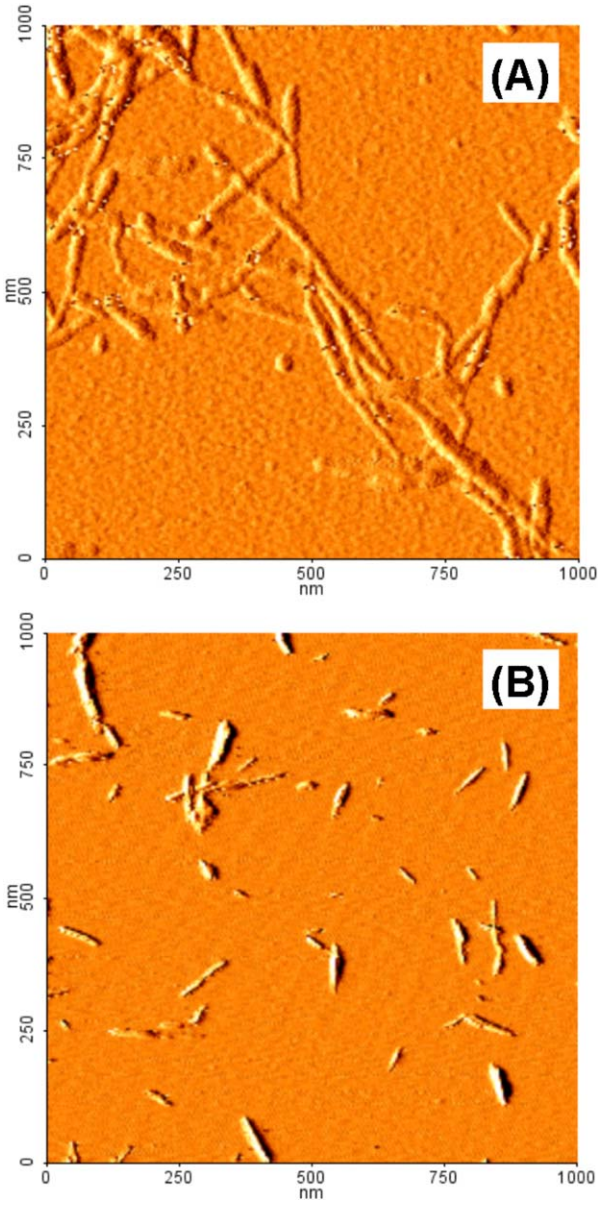

Figure 1. AFM images of (A) switchgrass CNC and (B) cotton CNC. [Color figure can be viewed in the online issue, which is available at wileyonlinelibrary.com.]

Rheological Measurements. Both steady and dynamic shear tests were performed on a stress-controlled rheometer (AR-G2, TA Instruments, USA) equipped with a plate-plate fixture of 60 mm in diameter. The steady shear data were collected from shear rate tests ranging from 0.01 to 1000 s^{-1}. For dynamic tests, the strain sweep was conducted with a frequency of 10 rad s^{-1} by varying strain from 0.01 to 100% to find the linear viscoelastic region, and the frequency sweep was performed from 0.01 to 100 rad s^{-1} at a strain amplitude within the linear viscoelastic region of 5%. All experiments were carried out at a constant temperature of 25°C. A vapor trap was used to prevent water evaporation in test process.

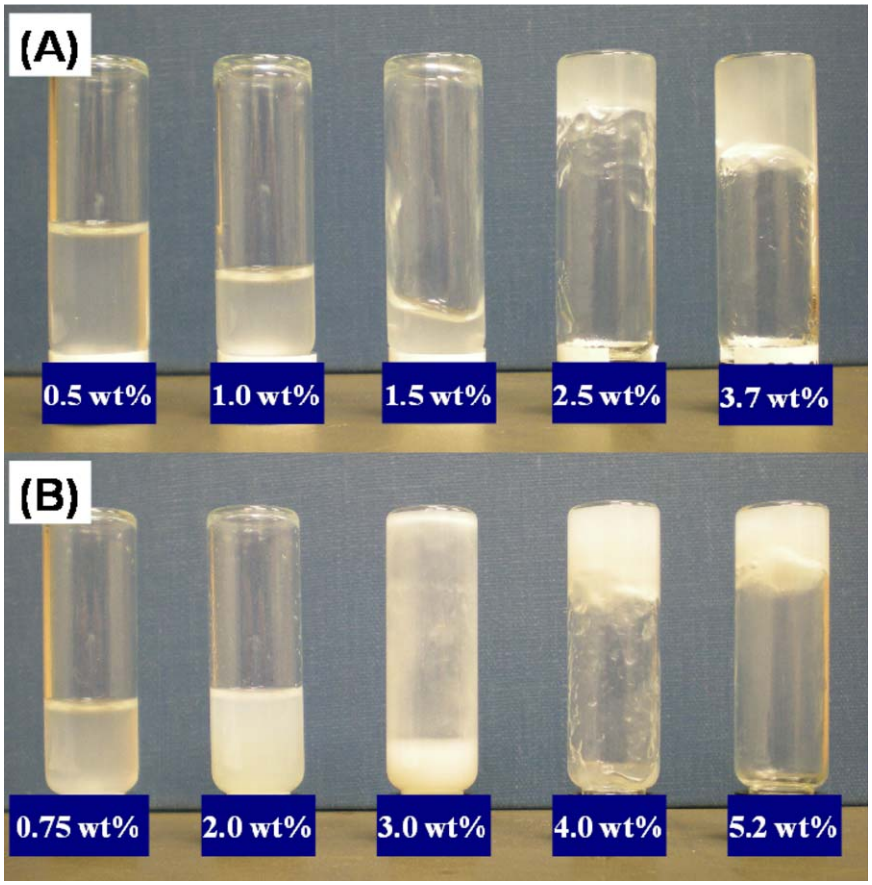

Figure 2. Photographs of (A) switchgrass CNC and (B) cotton CNC suspensions at different CNC concentrations. [Color figure can be viewed in the online issue, which is available at wileyonlinelibrary.com.]

RESULTS AND DISCUSSION

Steady Rheological Behavior

Figure 2(A) shows the switchgrass CNC suspensions at different concentrations. When CNC concentration (C) < 1.5 wt %, the switchgrass CNC suspension existed in a viscous liquid state, while in the regime of $C > 1.5$ wt % the suspensions existed in a gel-like state. Figure 2(B) shows the cotton CNC suspensions, which formed a gel when $C > 3.0$ wt %. Switchgrass CNC suspensions formed a gel at lower CNC concentrations than the cotton CNC suspensions due to its higher aspect ratio.

Figure 3(A) shows apparent viscosity (η_a) as a function of shear rate ($\dot{\gamma}$) for different concentrations of switchgrass CNC aqueous suspension at 25°C. At low concentrations ($C < 0.5$ wt %), the viscosity curves showed a Newtonian plateau at a low shear rate and displayed shear thinning behavior at the critical shear rate ($\dot{\gamma}_c$). According to Bercea's study,[30] CNCs keep random orientation at Newtonian plateau, thus, CNC suspension was in isotropic state when $C < 0.5$ wt %. At higher concentrations ($C > 0.5$ wt %), viscosity curves did not show a Newtonian plateau and displayed shear thinning behavior in all shear rate regions. It was suggested that CNC suspension entered into other phase state when $C > 0.5$ wt %, which will be discussed in the following section. As switchgrass CNC concentration increased, η_a increase and the shear thinning behavior become stronger. As can be seen in Figure 3(B), cotton CNC aqueous suspensions shows similar viscosity curves; however, the critical concentration of the cotton CNC suspensions is higher than that of the switchgrass CNC suspensions.

Figure 4 presents the viscosity of switchgrass and cotton CNC suspensions at same concentrations. It can be seen that the viscosity of switchgrass CNC suspension was much higher than that of cotton CNC suspension with same concentration. Moreover, switchgrass CNC suspension showed strong shear thinning behavior at 0.5 wt %, while cotton CNC suspension performed obvious shear thinning behavior at concentration of 1.5 wt %, which was much higher than that of switchgrass CNC suspension. This phenomenon was attributed to swtichgrass CNC having higher aspect ratio and lower critical overlap concentration.

To study the influence of CNC concentration on a suspension's steady rheological parameter, the dependence of η_a at different shear rates and non-Newtonian index (n) on CNC concentrations is shown in Figure 5. n was calculated using Carreau model by TA software from Figure 3. Carreau function[37] can be written as $\eta = \frac{\eta_0}{[1+(\lambda\dot{\gamma})^2]^{(1-n)/2}}$, where η_0 is zero shear viscosity and λ is relaxation time. According to the change in slope of $\eta_a \sim c$ and $n \sim c$, the viscosity data and n can be divided into three

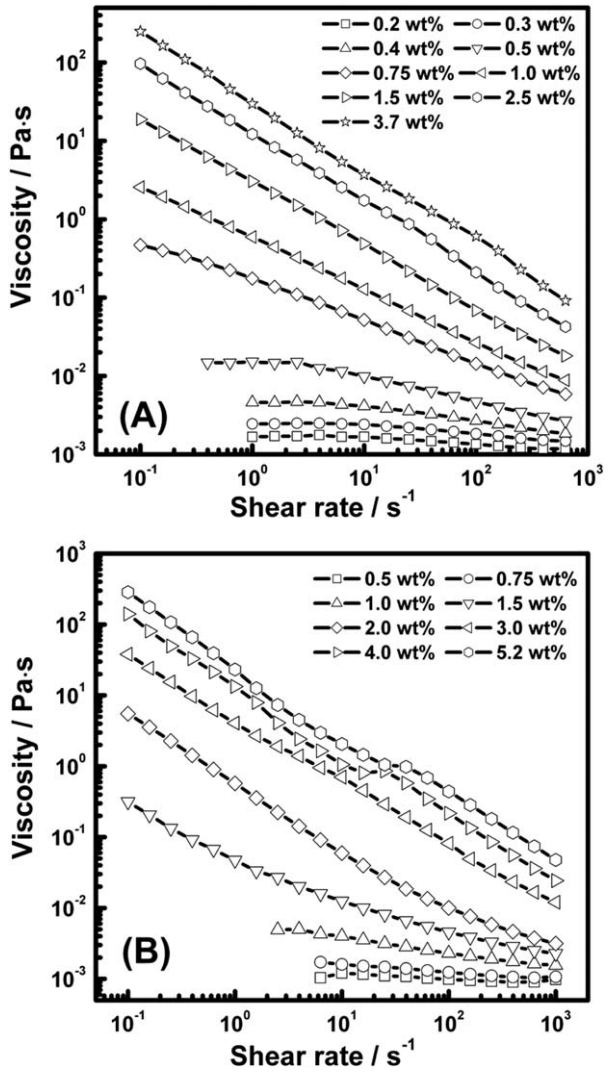

Figure 3. Apparent viscosity (η_a) as a function of shear rates ($\dot{\gamma}$) for (A) switchgrass CNC and (B) cotton CNC aqueous suspensions with different CNC concentrations at 25°C.

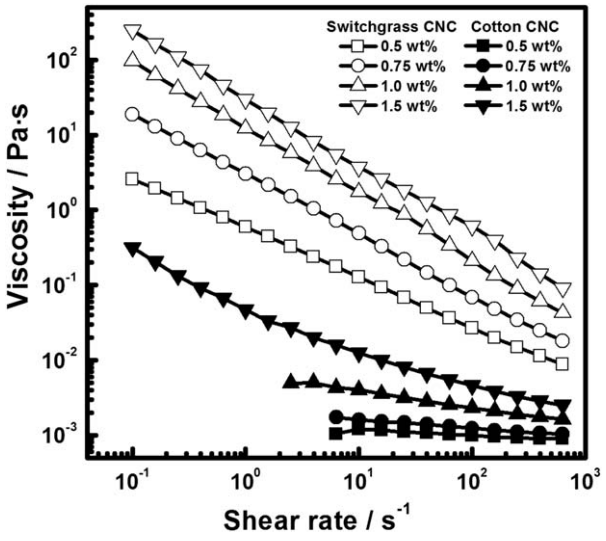

Figure 4. Apparent viscosity comparison of swichgrass CNC and cotton CNC suspensions at same concentrations. The open symbols represent switchgrass CNC suspension and the solid symbols denote cotton CNC suspension.

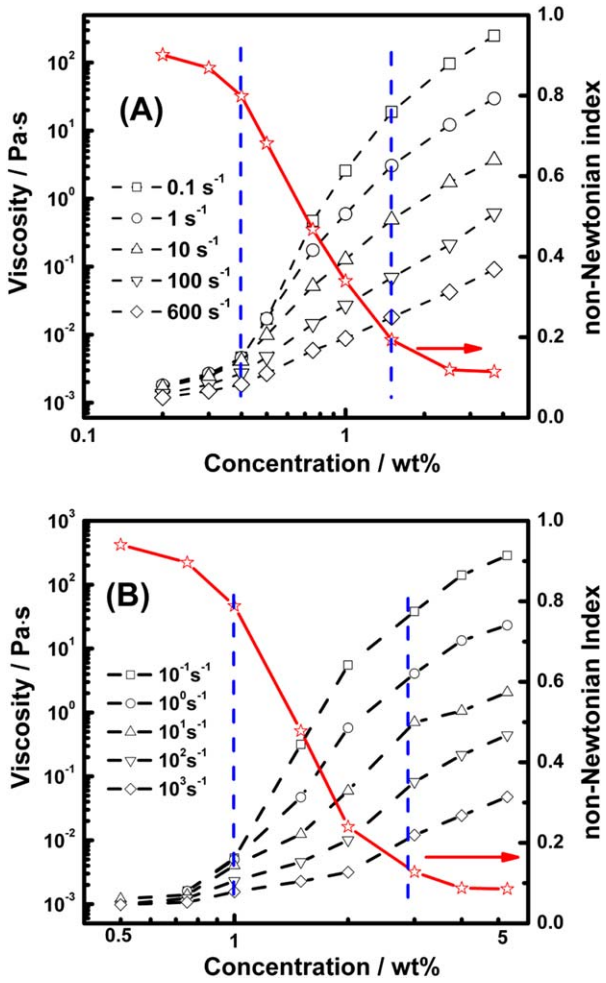

Figure 5. Dependence of apparent viscosity (η_a) at different shear rates and non-Newtonian index (n) on CNC concentrations, (A) switchgrass CNC and (B) cotton CNC suspensions. [Color figure can be viewed in the online issue, which is available at wileyonlinelibrary.com.]

parts in Figure 5(A). The two critical concentrations are defined as C_1 and C_2 (0.4 wt % and 1.5 wt %), which demonstrates that switchgrass CNC suspensions may correspond to three kinds of phase states in different concentration regions. In the first regime ($C < 0.4$ wt %), the viscosity increased slightly with concentration and n was close to 1. As discussed above, CNCs in this region showed Newtonian plateau in Figure 3(A) and performed isotropic in the suspension in the first regime. In the middle regime (0.4 wt % $< C <$ 1.5 wt %), the viscosity increases sharply, especially at low shear rates, and n decreased with increasing concentration. As CNC increasing at a critical concentration, CNC suspension would enter into biphasic state from isotropic state, namely, some CNCs form liquid crystalline and the other CNCs remain in the isotropic phase.[31] Therefore, an increase in CNC concentration has two effects on the rheological behavior of CNC suspensions: first, it acts to increase the viscosity of CNC suspensions due to an increase in the collision frequency of CNC particles; at the same time, it decreases

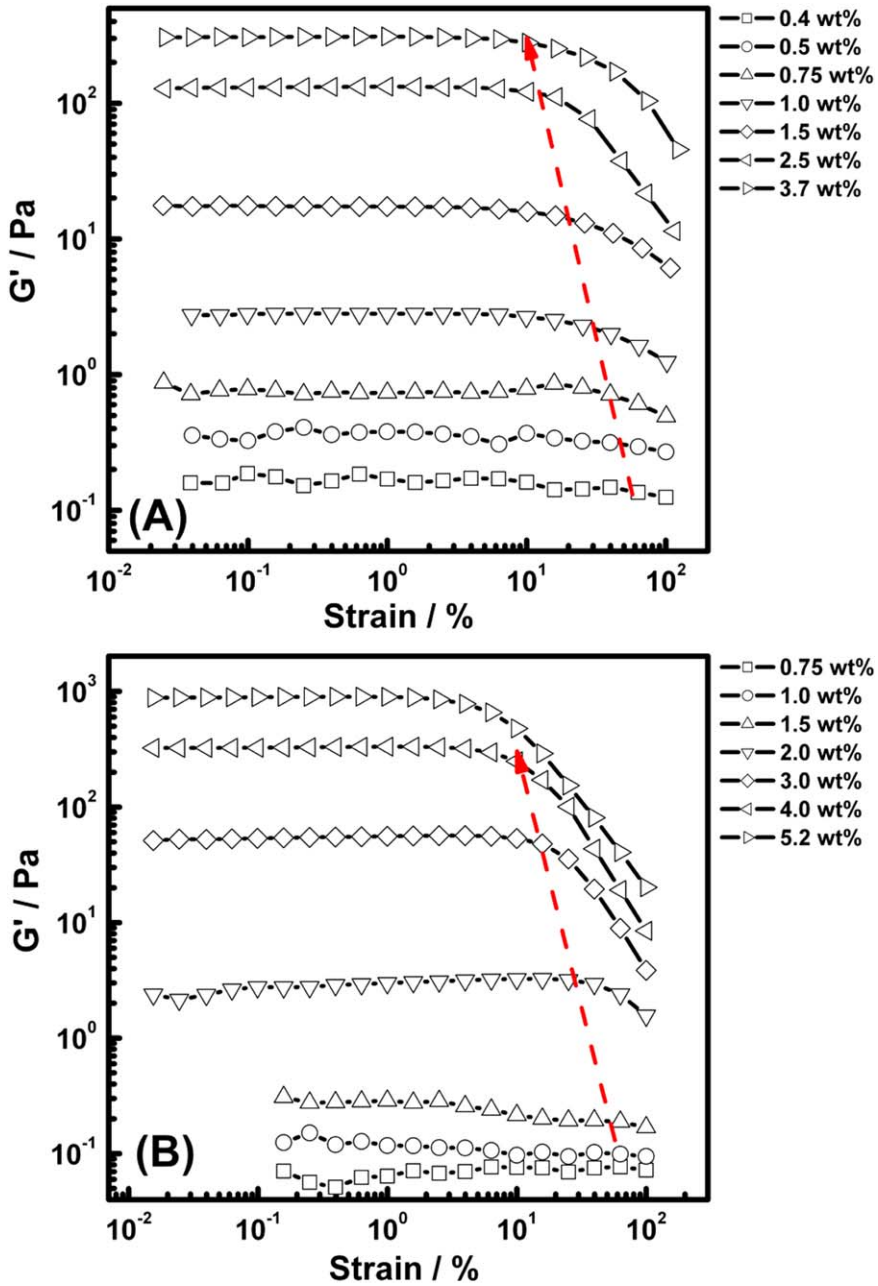

Figure 6. Dependence of dynamic storage modulus (G') on strain amplitude for different concentrations of (A) switchgrass CNC and (B) cotton CNC suspensions at 25°C and 10 rad s^{-1}. [Color figure can be viewed in the online issue, which is available at wileyonlinelibrary.com.]

the viscosity as liquid crystalline structures are formed. As CNC concentration continue increasing, all CNCs would orientate and form liquid crystalline. The whole rheological behavior of a liquid crystal suspension would initially increase its viscosity, then decrease, and finally increase again as the concentration rose. However, in our study, viscosity increased sharply as concentration increased and did not exhibit decreasing viscosity. In the third regime ($C > 1.5$ wt %), the change in viscosity and n slows as concentration increases and the slopes of viscosity and concentration at different shear rates become nearly identical. According to Figure 2, the third regime should correspond to a gel structure.

Bercea and Navard[30] studied the viscosity of high aspect ratio (140) tunicate CNC suspensions, and observed viscosity decreasing behavior at concentration of 0.6 vol % (0.9 wt %). Urena-Benavides[31] studied the viscosity of cotton CNC with aspect ratio of 12, showed viscosity decrease at concentration of 12.6 vol % (17.8 wt %). The aspect ratios of CNCs are 39 and 13 in our study respectively, but CNC suspension formed gel at low concentration (1.5 wt %), which demonstrated that the CNC concentration in our study is not high enough to show viscosity decreasing region. Therefore, the CNC suspension stayed in biphasic state before formed gel in the middle regime (0.4 wt % $< C <$ 1.5 wt %).

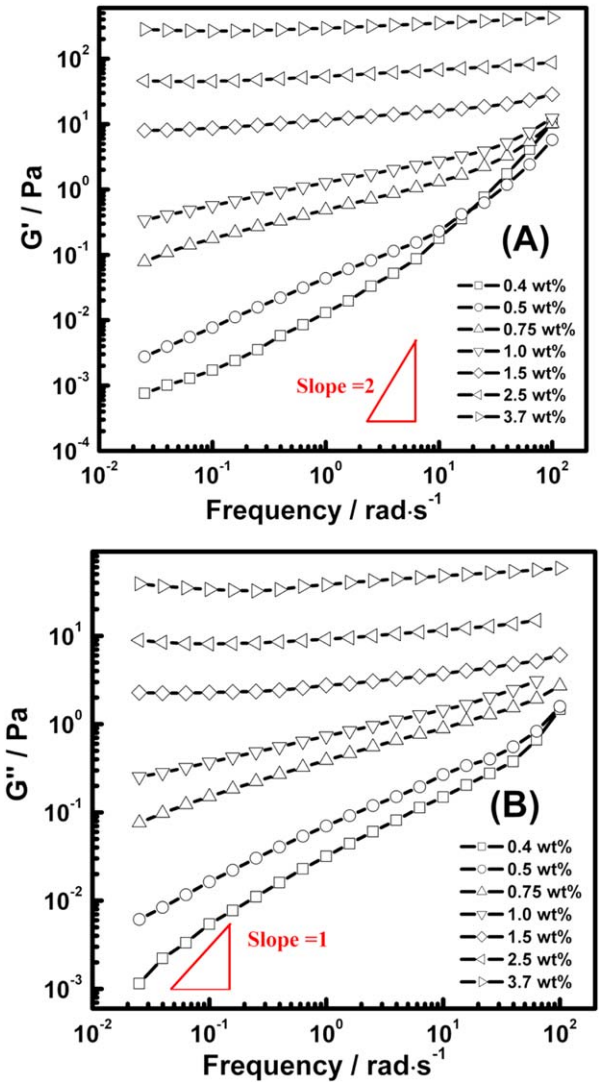

Figure 7. Plots of (A) storage modulus (G') and (B) loss modulus (G'') versus ω for switchgrass CNC suspensions with different concentrations at 5% strain at 25°C. [Color figure can be viewed in the online issue, which is available at wileyonlinelibrary.com.]

Figure 5(B) shows the dependence of η_a and n on concentration for cotton CNC suspensions. The curves of $\eta_a \sim C$ and $n \sim C$ can also be divided into three parts with two critical CNC concentration, which is similar as shown in Figure 5(A). The cotton and switchgrass CNC suspensions shows similar rheological behavior in Figures 3 and 5, demonstrated that the two aspect ratios (13 and 39) studied in this article do not influence the phase states of CNC in its suspension with concentration increasing. The difference is the two critical concentrations (C_1 and C_2). The C_1 and C_2 were 1.0 and 3.0 wt % for cotton CNC suspensions and higher than those of switchgrass CNC suspensions, which should be attributed to the lower aspect ratio of cotton CNC.

The critical overlap concentration of rod-like CNCs can be calculated by using the rod approximation,[38] the transition concentration of dilute and semidilute solution, $\Phi^* = d^2/L^2$, where Φ^* is volume concentration. The densities $\rho_{CNC} = 1.52$ g cm^{-3} and $\rho_{water} = 1.0$ g cm^{-3} are used to convert Φ^* to weight concentration (C^*). Based on the aspect ratios of the CNCs examined in our study, the C^* for switchgrass and cotton CNC suspensions were 0.1 and 0.9 wt %, respectively. The first critical concentrations (C_1) of CNC suspension from Figure 5 were 0.4 and 1.0 wt % for switchgrass and cotton CNC suspensions, which are very close to C^*. Thus, it suggested that C_1 may correspond to the critical overlap concentration. The second CNC critical concentration C_2 of switchgrass and cotton was 1.5 and 3.0 wt %. These concentrations represent those required for gel formation and suggested higher aspect ratio of CNC can form gel at lower concentration. It is noting that C_2 in our study were much lower than the 23 wt % observed in Urena–Benavides's study.[31] This may be attributed to the preparation method of CNC suspension for Urena–Benavides's and our studies. Urena–Benavides evaporated water to prepare CNC suspension with certain concentration, while we freeze-dried the CNCs and

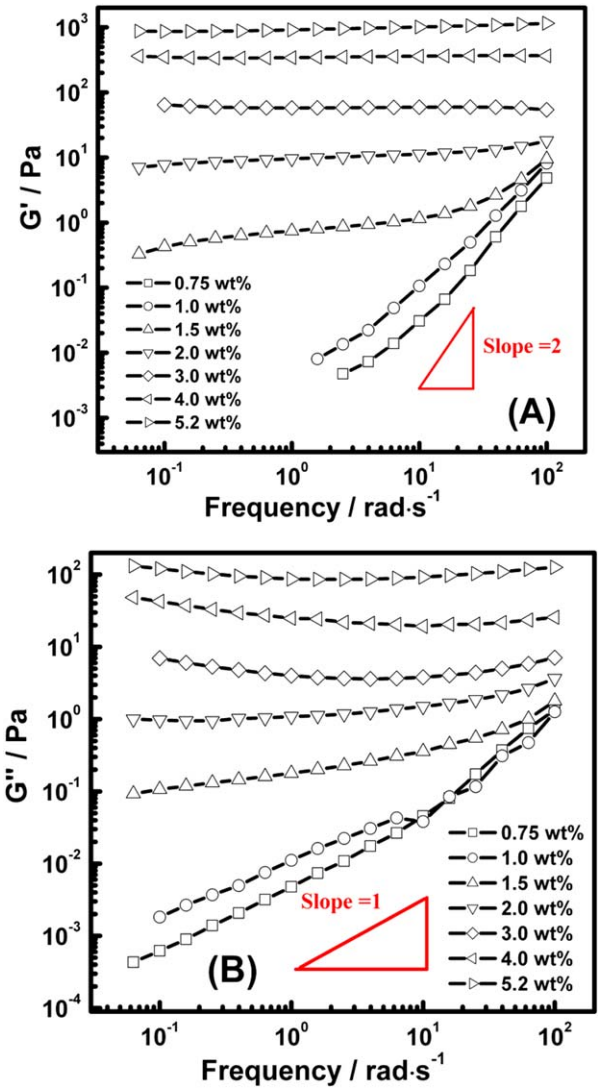

Figure 8. Plots of (A) storage modulus (G') and (B) loss modulus (G'') versus ω for cotton CNC suspensions with different concentrations at 5% strain at 25°C. [Color figure can be viewed in the online issue, which is available at wileyonlinelibrary.com.]

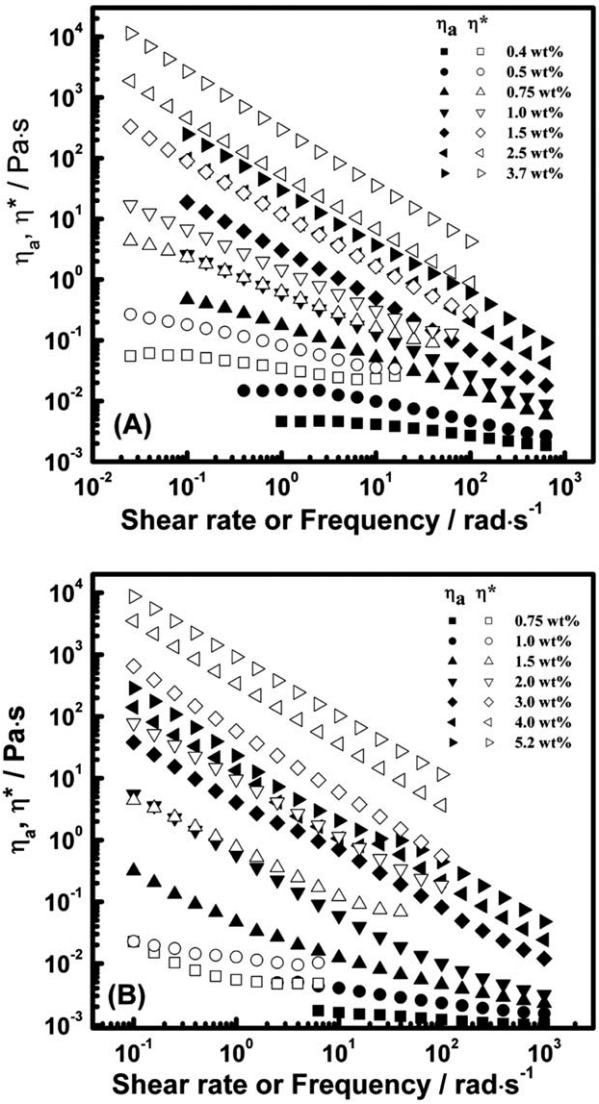

Figure 9. Cox–Merz rule comparison of (A) swichgrass CNC and (B) cotton CNC suspensions. The open symbols represent the steady shear viscosity (η_a) and the solid symbols denote complex viscosity (η^*).

then prepared a CNC suspension by adding CNCs to water and sonicating them.

Dynamic Rheological Behavior

Figure 6 shows the dependence of the dynamic storage modulus (G') on strain amplitude measured at 25°C and 10 rad s^{-1} for different concentrations of switchgrass CNC and cotton CNC suspensions. Linear viscoelastic behavior corresponding to strain-independent G' was observed at small strain amplitudes for all samples. It was also found that the critical strain decreased as the concentration of CNCs increased. As shown in Figure 6, a strain of 5% used in frequency (ω) sweep guaranteed the appearance of linear viscoelasticity under the conditions tested.

Figure 7 gives the plots of G' and loss modulus (G'') vs. ω for switchgrass CNC suspensions with different concentrations under 5% strain at 25°C. Both G' and G'' were observed to increase as CNC concentration increased, while the slopes of G' vs. ω and G'' vs. ω decreased as concentration increased to 1.5 wt %. Generally, in oscillation rheology test, ideal liquid would perform $G' \infty \omega^2$ and $G'' \infty \omega$ scaling relationships at low frequency regime. However, even at a switchgrass CNC suspension concentration of 0.4 wt %, the scaling index of G' and ω was smaller than 2, demonstrating that the switchgrass CNC system exhibited more rigidity than ideal liquid. As discussed above, some CNCs began to orientate when $C > 0.4$ wt %; therefore, this phenomenon may be attributed to the increasing ratio of liquid crystal structure in the CNC suspension. Urena–Benavides[16] and Liu's[17] studies showed a similar dynamic rheological behavior. When concentration was higher than 1.5 wt %, the slopes of both G' vs. ω and G'' vs. ω did not change with concentration and almost equaled zero. This should be attributed to the hydrogel structure of the CNC suspension. Cotton CNC suspensions show similar dynamic rheological behavior in Figure 8.

Cox–Merz Rules

The Cox–Merz rule is an empirical law stating that the steady shear rate viscosity (η_a) is equal to the complex viscosity (η^*) when the values of the shear rate and the oscillation frequency are equal. However, from Figure 9, it can be seen that both switchgrass CNC and cotton CNC suspension do not follow the Cox–Merz rule, as η^* was higher than η_a, in all CNC concentration regimes. Urena–Benavides's study[31] showed similar results, suggesting that the deviation from the Cox–Merz rule could be attributed to the liquid crystal domain present in the suspensions.

CONCULSIONS

Both switchgrass and cotton CNC suspensions displayed three different regimes in a viscosity–concentration graph, with the two critical concentrations corresponding to the overlap and gelation concentrations. The critical overlap and gelation concentrations were greatly influenced by CNC aspect ratio. Because of its higher CNC aspect ratio, the switchgrass CNC suspension formed a liquid crystal structure and formed a hydrogel at lower concentrations than the cotton CNC suspension.

ACKNOWLEDGMENTS

This work was financially supported by the Natural Science Foundation of Zhejiang Province (LQ12C16003), the Pre-research Project of Research Center of Biomass Resource Utilization, ZAFU (2013SWZ02-2), the Zhejiang Provincial Top Key Discipline of Wood Science and Technology (No. 201109), and the UTIA 2013 Innovation Grant and Tennessee Experimental Station Project #TEN00422.

REFERENCES

1. Samir, M.; Alloin, F.; Dufresne, A. *Biomacromolecules* **2005**, *6*, 612.
2. Habibi, Y.; Lucia, L. A.; Rojas, O. J. *Chem. Rev.* **2010**, *110*, 3479.
3. Eichhorn, S. J. *Soft Matter* **2011**, *7*, 303.

4. Hirota, M.; Tamura, N.; Saito, T.; Isogai, A. *Cellulose* **2010**, *17*, 279.
5. Isogai, A.; Saito, T.; Fukuzumi, H. *Nanoscale* **2011**, *3*, 71.
6. Montanari, S.; Rountani, M.; Heux, L.; Vignon, M. R. *Macromolecules* **2005**, *38*, 1665.
7. Filson, P. B.; Dawson-Andoh, B. E.; Schwegler-Berry, D. *Green Chem.* **2009**, *11*, 1808.
8. Ahola, S.; Turon, X.; Osterberg, M.; Laine, J.; Rojas, O. J. *Langmuir* **2008**, *24*, 11592.
9. Filson, P. B.; Dawson-Andoh, B. E. *Bioresour. Technol.* **2009**, *100*, 2259.
10. Man, Z.; Muhammad, N.; Sarwono, A.; Bustam, M. A.; Kumar, M. V.; Rafiq, S. *J. Polym. Environ.* **2011**, *19*, 726.
11. Tang, L.; Huang, B.; Ou, W.; Chen, X.; Chen, Y. *Bioresour. Technol.* **2011**, *102*, 10973.
12. Beck-Candanedo, S.; Roman, M.; Gray, D. G. *Biomacromolecules* **2005**, *6*, 1048.
13. Rahimi, M.; Behrooz, R. *Int. J. Polym. Mater.* **2011**, *60*, 529.
14. Lu, P.; Hsieh, Y. *Carbohydr. Polym.* **2011**, *87*, 564.
15. Brito, B. S. L.; Pereira, F. V.; Putaux, J. L.; Jean, B. *Cellulose* **2012**, *19*, 1527.
16. van den Berg, O.; Capadona, J. R.; Weder, C. *Biomacromolecules* **2007**, *8*, 1353.
17. Sturcova, A.; Davies, G. R.; Eichhorn, S. *J. Biomacromolecules* **2005**, *6*, 1055.
18. Wu, Q.; Meng, Y.; Concha, K.; Wang, S.; Li, Y.; Ma, L.; Fu, S. *Ind. Crop. Prod.* **2013**, *48*, 28.
19. Meng, Y.; Wu, Q.; Wang, S.; Young, T. M.; Huang, B.; Li, Y. *European Polym. J.* (in Review).
20. Favier, V.; Chanzy, H.; Cavaille, J. Y. *Macromolecules* **1995**, *28*, 6365.
21. Helbert, W.; Cavaille, J. Y.; Dufresne, A. *Polym. Compos.* **1996**, *17*, 604.
22. Lu, P.; Hsieh, Y. L. *Nanotechnology* **2009**, *20*, 415604.
23. Gray, D. G. *Cellulose* **2008**, *15*, 297.
24. Oksman, K.; Mathew, A. P.; Bondeson, D.; Kvien, I. *Compos. Sci. Technol.* **2006**, *66*, 2776.
25. Bahar, E.; Ucar, N.; Onen, A.; Wang, Y.; Oksuz, M.; Ayaz, O.; Ucar, M.; Demir, A. *J. Appl. Polym. Sci.* **2012**, *125*, 2882.
26. Ben Elmabrouk, A.; Thielemans, W.; Dufresne, A.; Boufi, S. *J. Appl. Polym. Sci.* **2009**, *114*, 2946.
27. Xiang, C. H.; Taylor, A. G.; Hinestroza, J. P.; Frey, M. W. *J. Appl. Polym. Sci.* **2013**, *127*, 79.
28. Podsiadlo, P.; Sui, L.; Elkasabi, Y.; Burgardt, P.; Lee, J.; Miryala, A.; Kusumaatmaja, W.; Carman, M. R.; Shtein, M.; Kieffer, J.; Lahann, J.; Kotov, N. A. *Langmuir* **2007**, *23*, 7901.
29. Csoka, L.; Hoeger, I. C.; Rojas, O. J.; Peszlen, I.; Pawlak, J. J.; Peralta, P. N. *Acs Macro Lett.* **2012**, *1*, 867.
30. Bercea, M.; Navard, P. *Macromolecules* **2000**, *33*, 6011.
31. Urena-Benavides, E. E.; Ao, G.; Davis, V. A.; Kitchens, C. L. *Macromolecules* **2011**, *44*, 8990.
32. Liu, D.; Chen, X.; Yue, Y.; Chen, M.; Wu, Q. *Carbohydr. Polym.* **2011**, *84*, 316.
33. Gong, G.; Mathew, A. P.; Oksman, K. *Tappi J.* **2011**, *10*, 7.
34. Araki, J.; Wada, M.; Kuga, S.; Okano, T. *Colloids Surf. Physicochem. Eng. Aspects* **1998**, *142*, 75.
35. Boluk, Y.; Lahiji, R.; Zhao, L.; McDermott, M. T. *Colloids Surf. Physicochem. Eng. Aspects* **2011**, *377*, 297.
36. Simha, R. *J. Phys. Chem.* **1940**, *44*, 25.
37. Carreau, P. J.; De Kee, D. C. R.; Chhabra, R. P. Rheology of Polymeric Systems Principles and Application; Hanser publishers: New York, **1997**.
38. Doi, M.; Edwards, J. F. The Theory of Polymer Dynamics; Clarendon Press: Oxford, U.K., **1986**; Chapter *8*, p 289.